Water Research 305 (2026) 126485

Contents lists available at ScienceDirect

Water Research

journal homepage: www.elsevier.com/locate/watres

Wastewater viromics reveals host-structured viral signals and non-human pathogens

Jaana Jurvansuu [a], Eevi Sipponen [a], Elisa Salmivirta [b], Kirsi-Maarit Lehto [a], Aki Havulinna [c,d], Tarja Pitkänen [b,e], Sami Oikarinen [a,*]

[a] Faculty of Medicine and Health Technology, Tampere University, Tampere, Finland
[b] Public Health Department, Microbiology Unit, Finnish Institute for Health and Welfare, Kuopio, Finland
[c] Department of Computing, University of Turku, Turku, Finland
[d] Research Program for Clinical and Molecular Metabolism, Faculty of Medicine, University of Helsinki, Helsinki, Finland
[e] Faculty of Veterinary Medicine, Department of Food Hygiene and Environmental Health, University of Helsinki, Helsinki, Finland

HIGHLIGHTS

- Wastewater reveals diverse non-human viral signals.
- Host-linked viral patterns reflect regional animal populations.
- Wastewater supports One Health surveillance of animal and plant pathogens.

GRAPHICAL ABSTRACT

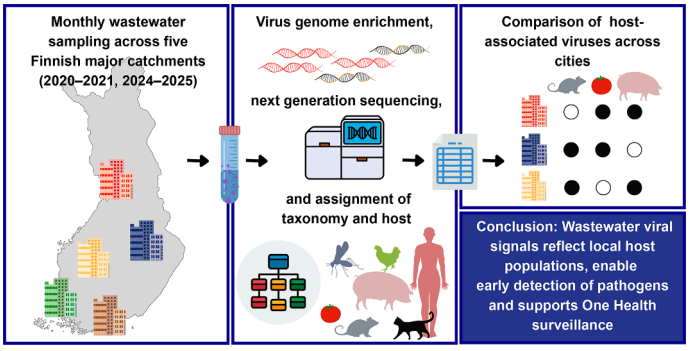

ARTICLE INFO

Keywords:
Wastewater viromics
Environmental surveillance
Metagenomics
One-health

ABSTRACT

Wastewater represents a powerful platform for human virus surveillance. However, the entry of animal- and plant-associated viruses into sewage is heterogeneous and incompletely understood, creating uncertainty about how reliably wastewater reflects non-human virus circulation. Here, we address this by analysing monthly wastewater metagenomic data from two distinct periods (2020–2021 and 2024–2025) across five major Finnish wastewater treatment plant catchments using a targeted hybrid-capture approach to characterise the composition, host range, and spatial distribution of the non-human wastewater virome. Nearly half of the detected viral accessions were non-human, indicating substantial diversity, despite human-associated viruses accounting for 83% of normalised viral reads. Rodent-, livestock-, and bird-associated viruses showed spatial structuring consistent with regional host populations. The wastewater viromics also detected four EU-regulated plant pathogens, including tomato brown rugose fruit virus, which was highly prevalent in wastewater two years before its first official detection in Finland. Together, these results show that wastewater contains structured, host-linked viral signals, supporting its use as an ecological proxy for non-human virus circulation.

* Corresponding author.
E-mail address: sami.oikarinen@tuni.fi (S. Oikarinen).

https://doi.org/10.1016/j.watres.2026.126485
Received 17 April 2026; Received in revised form 2 July 2026; Accepted 10 July 2026
Available online 11 July 2026
0043-1354/© 2026 The Authors. Published by Elsevier Ltd. This is an open access article under the CC BY license (http://creativecommons.org/licenses/by/4.0/).

1. Introduction

Wastewater aggregates biological signals shed by large populations, enabling sensitive detection of public health threats independent of individual clinical testing and inclusive of both symptomatic and asymptomatic infections. Wastewater-based epidemiology originated as a tool for monitoring illicit drug use and enteric pathogens but expanded during the COVID-19 pandemic to include major respiratory viruses (Naughton et al., 2023; Zhang et al., 2024). SARS-CoV-2 wastewater surveillance anticipated case trends and detected viral circulation during periods of reduced testing, demonstrating wastewater as a robust, unbiased, and passive indicator of community infection dynamics (Robins et al., 2022).

Most existing wastewater surveillance frameworks are optimised for specific human viruses. Human-associated viral signals in municipal wastewater are introduced primarily through toilet waste and household "greywater". Human viruses reach sewers via faeces and urine, and also through skin, saliva, sputum/mucus/phlegm, which are flushed or washed into drains during hygiene activities aggregating multiple shedding routes into a single composite sample (Crank et al., 2022; Jones et al., 2020; Zahedi et al., 2021). Beyond targeted pathogen monitoring, advances in virus enrichment and high-throughput sequencing have enabled characterisation of the broader human wastewater virome (Bibby and Peccia, 2013; Tisza et al., 2023). This has motivated proposals for virome-scale wastewater monitoring as a core component of public-health surveillance and pandemic-preparedness systems (Clark et al., 2023).

Recent work has shown that wastewater viromes are not exclusively human in origin. Metagenomic studies have identified a wide range of non-human viruses of eukaryotic hosts in urban wastewater, including viruses associated with domesticated animals, wildlife, plants, and environmental reservoirs (Karatas et al., 2025; Worp et al., 2025). These findings highlight wastewater as a unique interface for One Health surveillance, capturing viral signals from human, animal, and plant sources within shared ecosystems. Despite these advances, non-human components of the wastewater virome remain comparatively underexplored relative to human pathogens.

Non-human viruses enter wastewater through several non-exclusive input pathways that connect urban catchments to animals, plants, and environmental reservoirs. Plant viruses are introduced to sewage mainly through diet and food handling and waste; Pepper mild mottle virus (PMMoV) is an example where high wastewater abundance is explained largely by dietary origin from peppers and processed pepper products (Kitajima et al., 2018; Symonds et al., 2019). Broader wastewater virome surveys repeatedly detect diverse plant- and environment-associated viral taxa, consistent with inputs from kitchens, food-processing streams, and agricultural runoff (Chahal et al., 2016; Duarte et al., 2023; Lopez-Roblero et al., 2024).

Animal-derived food sources, including livestock such as cattle and pigs, have also shown to contribute viral material to wastewater through food processing, preparation, and waste streams (Al-Gheethi et al., 2023; dos Santos et al., 2011). In addition to food-derived inputs, animal-associated viral material can enter wastewater through urban wildlife and infrastructure-mediated pathways. Urban sewer systems are inhabited by synanthropic wildlife, particularly rodents such as *Rattus norvegicus*, which shed faeces and urine directly within sewer infrastructure and are known reservoirs for multiple vertebrate-associated viruses (Firth et al., 2014; Himsworth et al., 2013). Rain-driven runoff transports faecal material from pets, other domestic animals, and urban wildlife into urban drainage networks, as demonstrated by microbial source tracking studies of stormwater runoff (Lancaster et al., 2024; Mallin et al., 2009; Monteiro et al., 2021; Sherchan et al., 2022). During wet-weather conditions, interactions between stormwater and sanitary sewer systems, combined with sewer leakage and exfiltration, allow animal-derived and environmental microbial material to mix with wastewater (Adriaenssens et al., 2021; Sidhu et al., 2013).

The entry of animal- and plant-associated viruses into sewage is heterogeneous and incompletely understood, creating uncertainty about how reliably wastewater reflects non-human virus circulation. Here, we address this by analysing two years of monthly wastewater samples from five major Finnish wastewater treatment plant catchments to characterise the composition, host range, and spatial variation of the non-human wastewater virome.

2. Materials and methods

2.1. Wastewater sample collection, processing, and nucleic acid extraction

Wastewater samples were collected monthly from April 2020 to March 2021 and April 2024 to March 2025 from the main wastewater treatment plants of Helsinki, Kuopio, Tampere, Turku, and Oulu. Each site contributed a 24-h composite wastewater sample collected from Sunday to Monday on the same calendar date, resulting in a total of 120 wastewater samples. The wastewater treatment plants serve altogether 1,651,000 people covering 29% of the Finnish population (Fig. 1). Samples were shipped and stored at +4 °C for 1–2 days prior to processing. Samples collected in 2020–2021 were stored at −20 °C for up to five years before concentration, whereas samples from 2024–2025 were concentrated directly from +4 °C storage. Concentration of the samples followed protocol previously described in Sarekoski et al., 2024, with modifications. Briefly, 80 mL of wastewater was centrifuged at 4,654×g for 30 min. The resulting pellet was resuspended in 1 mL of supernatant, and 350 µL of the suspension was transferred to a new tube, mixed with 150 µL of 2 × DNA/RNA Shield, and stored at −80 °C. Cell and viral particle lysis was performed by bead beating for 1 min at full power using a Mini-Beadbeater-24 in 500 µL of Viral300 DNA/RNA Kit lysis buffer. Beads were pelleted, and the supernatant was centrifuged at 12,000×g for 5 min. Clarified supernatants were subjected to nucleic acid extraction using the Viral300 DNA/RNA Kit on a chemagic 360 instrument following the manufacturer's protocol. PCR inhibitors were subsequently removed using the OneStep PCR Inhibitor Removal Kit according to the manufacturer's instructions. Purified nucleic acids were stored at −80 °C until library preparation, virome enrichment, and next-generation sequencing.

2.2. Library preparation, target enrichment, and sequencing

Nucleic acid concentrations were measured using a Qubit™ 3.0 Fluorometer with the RNA High-Sensitivity Assay Kit. Library preparation was performed using the Twist Total Nucleic Acids Library Preparation EF Kit 2.0 for Viral Pathogen Detection. Samples were normalized to 3.3 ng/µL and reverse-transcribed to cDNA using the ProtoScript II First Strand cDNA Synthesis Kit, followed by second-strand synthesis with the NEBNext Ultra II Non-Directional RNA Second Strand Synthesis Module. Library construction included DNA purification, fragmentation, end repair, dA-tailing, ligation of Twist universal adapters, and indexing with Twist UDI primers. Final libraries were quantified and quality-checked using an Agilent 4150 TapeStation with the D1000 ScreenTape Assay to verify fragment size distributions (250–450 bp) and adequate library concentrations.

Following the eukaryotic wastewater virome enrichment approach described by Tisza et al. (2023), hybridization-based target enrichment was performed using the Twist Comprehensive Viral Research Panel following the Twist Target Enrichment Standard Hybridization v1 protocol. In contrast to the original protocol, 16 libraries were pooled together at equal mass instead of 8. For the samples collected in April-June 2020 the libraries were pooled at a total mass of 1,500 ng. The total mass of the pool was increased to 4,500 ng for the rest of the samples to ensure high enough end concentration of the final product. Enriched library pools were quantified using the TapeStation system and sequenced by Macrogen Europe (Amsterdam, Netherlands) on an

Illumina NovaSeq X platform, generating 2 × 150 bp paired-end reads. Negative controls were nuclease-free water carried through nucleic acid extraction, library preparation, hybrid capture, and sequencing. Positive controls were HCoV-229E and Coxsackievirus B4 spiked into pellet matrices, and both viruses were successfully detected. Sequencing results are deposited into NCBI Sequence Read Archive under BioProject ID PRJNA1421147, with access codes SAMN55289260-SAMN55289379.

2.3. Annotation of metagenome reads

Bioinformatic processing followed the pipeline for detection and quantification of human and animal viral pathogens from short-read metagenomic data described by Tisza et al. (Tisza et al., 2023). Raw read quality was assessed using FastQC (v0.11.9) and MultiQC (v1.19). Read trimming and contaminant filtering were performed using BBDuk and BBMap from the BBTools suite (v39.25). In detail, reads were quality trimmed (Q25), and adapters were removed using right-side trimming, k-mer length of 23 (minimum 11) with one allowed mismatch. Quality trimming was applied to both read ends and adapter overlap detection and paired-end consistency were enabled. Reads with length <50 bp or Phred score <23 after trimming were discarded. Human/PhiX reads were removed from the trimmed reads by aligning read to a combined human (GCF_000001405.40) and PhiX reference with BBMap default parameters. Alignment statistics for contaminant reads were evaluated with samtools (v1.21). Filtered paired-end reads were analysed using the EsViritu pipeline (v1.0.3) with default parameters against the EsViritu Virus Pathogen Database (v3.1.1). Viral abundance was estimated with normalised read count value, reads per kilobase of reference genome per million filtered reads (RPKMF). For segmented viruses, all genomic segments belonging to the same viral GenBank reference assembly were combined into a single viral assembly for analysis. RPKMF was then calculated using the combined length of all segments and the summed read counts across segments.

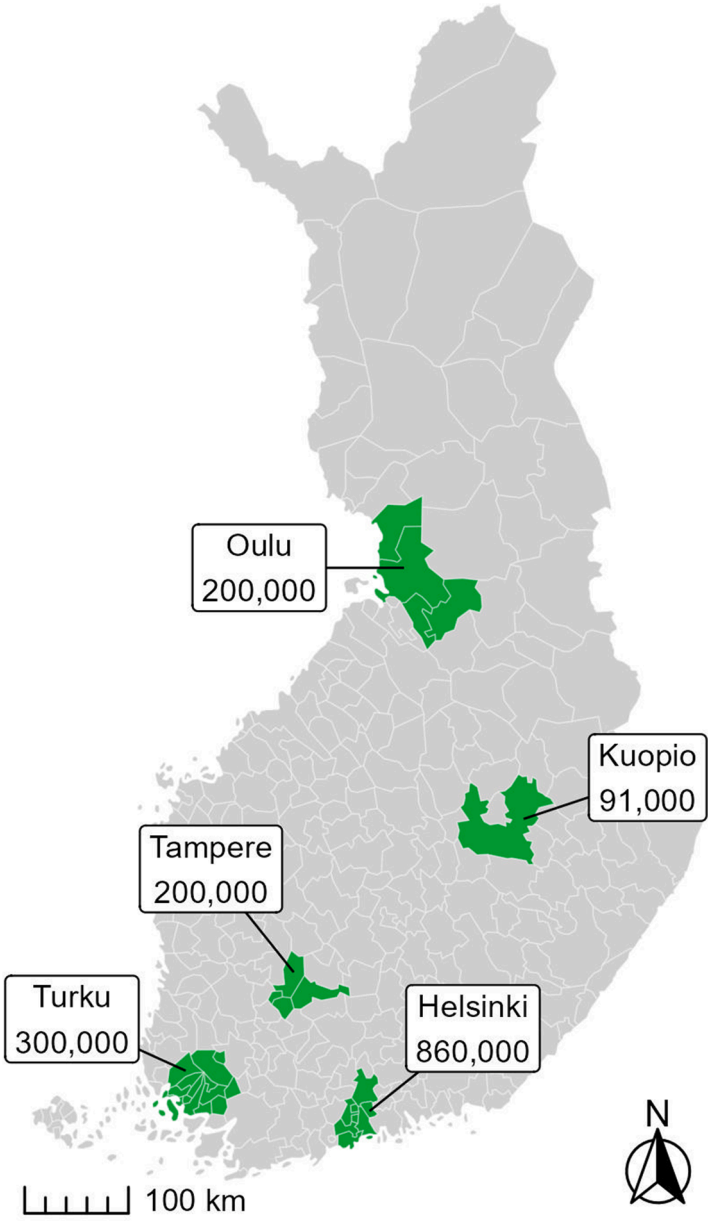

Fig. 1. Map of sampled wastewater treatment plants showing associated municipalities, city names, and population served. A 100-km scale bar and north arrow are provided.

2.4. Host assignment and genome type

Host attribution was performed using Python with the pandas library (v2.3.1) and Biopython Entrez (v1.85) (Cock et al., 2009). Host annotations were assigned at the accession level using host metadata associated with each GenBank accession to accommodate viruses reported from multiple hosts and capture the diversity of host records represented in the reference database. Unique GenBank accession numbers were queried against the NCBI Nucleotide database using the Entrez API (Sayers et al., 2020) to retrieve GenBank records and extract reported host metadata. When host information was missing, additional Entrez searches were conducted using virus names as query terms. All retrieved host strings were aggregated and, when multiple hosts were associated with an accession, the most frequently reported host was assigned as the consensus host by majority voting. Canonical taxa were identified by parsing species-level descriptors, and common names were mapped to scientific species using curated lookup tables. Remaining host names were resolved using the Global Names Verifier (GNverifier API; (Mozzherin, 2025)) followed by taxonomic classification with the GBIF Species Match API (GBIF Secretariat, 2023). Detections were assigned to the environmental source host category when the metadata associated with the matched GenBank accession indicated an environmental isolation source, such as sewage or soil. Unresolved taxonomic assignments were resolved manually based on accession-linked reference publications.

Two host assignments were manually corrected: Parvovirus NIH-CQV (NC_022089.1) was reassigned from human to unknown based on evidence of spin-column contamination (Naccache et al., 2014), and Gyrovirus GyV3 was reassigned as a chicken virus based on published evidence (Li et al., 2021). Host information for selected Torque teno viruses was additionally curated from accession reference publications. Detections annotated with host species *Homo sapiens* were excluded from the analyses. The host attribution script is available at GitHub (github.com/jjurvans/virome-host-resolver).

Virus genome types were assigned hierarchically, first at the family level and then at the order level, using the International Committee on Taxonomy of Viruses (ICTV) Virus Metadata Resource (VMR_MSL40.v1.20250307.xlsx).

The final dataset, including taxonomic, host, and genome type annotations, is available on GitHub (EsViritu_with_hosts_genome.tsv; https://github.com/jjurvans/wastewater-nonhuman-virome).

2.5. Data analysis and visualisation

Data analysis was performed in Python using pandas (v2.3.1), NumPy (v2.2.5), SciPy (v1.16.3), statsmodels (v0.14.5), and scikit-bio (v0.7.1). Data visualisation was conducted using matplotlib (v3.10.0). Analysis and visualization scripts are available on GitHub (github.com/jjurvans/wastewater-nonhuman-virome), where they can be executed directly via GitHub Codespaces. Map and hierarchical representations of detected viral species were generated in R (v4.5.1). Geographic visualisations were generated using the sf (v1.0.24) and ggspatial (v1.1.10) packages. Phylogenetic-style hierarchies were constructed using the *taxo2phylog* function from the ade4 package (v1.7.24) (Thioulouse et al., 2018) and visualized with ggtree (v3.16.3).

3. Results

3.1. Quality control and assessment of storage effects

Human adenovirus 2 (MT277585.1) and Cripavirus ropadi (NC_001874.1) were detected in two of the five negative controls (149 and 92 reads, respectively), consistent with low-level laboratory contamination, and were excluded from subsequent analyses. Because the 2020–2021 wastewater samples were stored frozen for five years, we tested for nucleic acid degradation during storage by comparing the samples from 2024–25 to those from 2020–21 for non-human viruses using sample-level RPKMF-normalised abundances and Mann–Whitney U tests with FDR correction. Only ssDNA(±) viruses differed significantly between the years ($q = 6.5 \times 10^{-4}$) (Table S1). These results indicated that there were no uniform RNA degradation during long-term freezing.

3.2. Host distribution and taxonomic diversity of non-human viruses

At the host kingdom level, the majority of unique virus assemblies (i.e., unique viral accession records after consolidation of segments belonging to the same reference assembly) were associated with animals (90.6%), followed by plants (8.6%), with less than 1% unassigned to any host and categorised as environmental source (primarily wastewater-associated viruses), and a single virus associated with protozoans (Fig. 2A). At the host genus level, humans and non-human hosts contributed approximately equal numbers of unique virus assemblies (Fig. 2B). In contrast, when considering reads per kilobase of reference genome per million filtered reads (RPKMF)-normalised read count, human-associated viruses dominated over non-human viruses (Fig. 2D). Among non-human hosts, the most common hosts by unique virus assemblies included pigs (*Sus*), chickens (*Gallus*), cattle (*Bos*), cats (*Felis*), dogs (*Canis*), *Capsicum* plants (bell and chili peppers), and pigeons (*Columba*), while bats (*Hipposideros*) and mosquitoes (*Culex*) contributed high read abundances. Consistent with these patterns, animal-associated viruses accounted for 98.2% of total read abundance at the host kingdom level, whereas plant-associated viruses contributed only 1.5% (Fig. 2C).

Across all wastewater samples, we identified 1,140 unique non-human viral assemblies corresponding to 460 virus species, 127 genera, 32 families, 23 orders, and 11 phyla. Unlike individual accessions, which represent single genomic segments or sequences, an assembly integrates all segments of a multisegmented virus into one strain-specific representation. The most represented virus families by number of assemblies were *Astroviridae* (144 assemblies), *Parvoviridae* (134), *Circoviridae* (116), *Coronaviridae* (84), and *Picornaviridae* (75) (Fig. 2E). The most prevalent viruses were Porcine picobirnavirus and Porcine stool-associated circular virus 4, each detected in 119 of 120 samples.

3.3. Read abundance, assembly coverage, and genomic composition of non-human viruses

Average read identity values for non-human viral detections were constrained by a minimum threshold of 80%, with a mean identity of 95.6% (SD 3.8) across all detections (Fig. 3A). Read counts were highly skewed, with a median of 18 reads (IQR 72) and a mean of 206 reads, reflecting a small number of high-count detections (Fig. 3B). Consistent with this pattern, more than 50% of detected virus genomes exhibited less than 10% assembly coverage (Fig. 3C). Percent of assembly coverage was strongly positively correlated with log-transformed read counts (Spearman $\rho = 0.64$, $p < 1 \times 10^{-16}$, $n = 6{,}939$), indicating that low assembly coverage was associated with low read count (Fig. 3D).

We analysed descriptively unique viral assembly counts across wastewater catchment areas (hereafter referred to by city) and seasons with samples from different sampling periods pooled together. This revealed temporal and spatial variation. Fewer unique assemblies were detected during winter months (October–March) compared with summer months (April–September), and the highest number of unique assemblies was observed in Turku, whereas Tampere and Oulu exhibited the lowest counts (Fig. 3E). Across all non-human assemblies, approximately half were positive-sense single-stranded RNA (+ssRNA) viruses, while roughly one quarter were single-stranded DNA (ssDNA) viruses (Fig. 3F).

When grouped by host class and genome type, non-human mammalian-associated viruses were the most abundant group, comprising 656 assemblies, nearly half of which were +ssRNA viruses

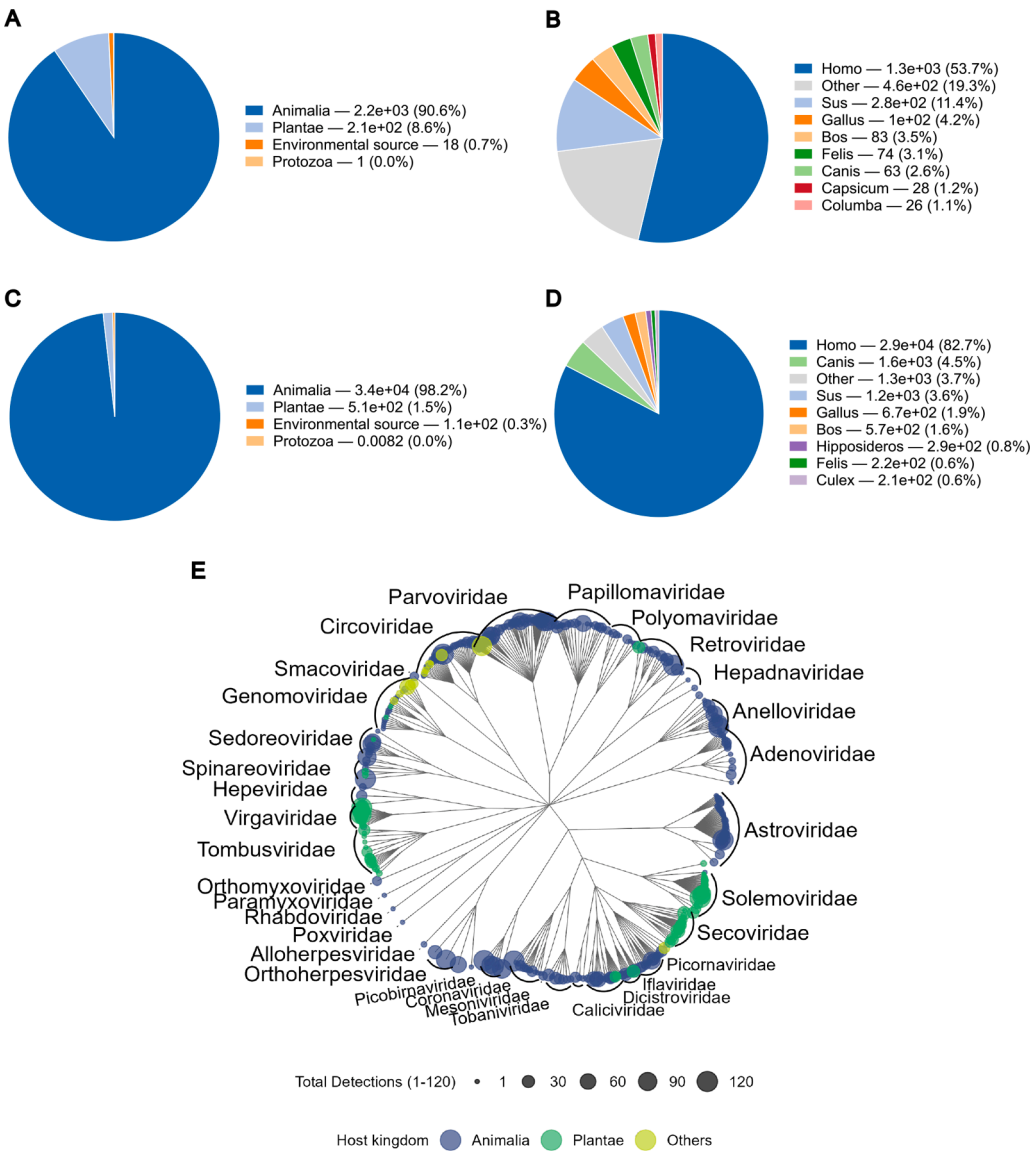

Fig. 2. Wastewater virome host categories and non-human virus taxonomy. (A) Host kingdom by number of unique assemblies. (B) Host genus by number of unique assemblies. (C) Host kingdom by summed RPKMF-normalised reads. (D) Host genus by summed RPKMF-normalised reads. Remaining categories are grouped as Other; percentages indicate the proportion of the total. (E) Detected viral species are displayed in a taxonomy-ordered hierarchical tree based on taxonomic ranks rather than phylogenetic relationships. Each tip represents a virus species, tip color the hosts kingdom and tip size reflects the number of wastewater samples in which that species was detected.

and approximately one quarter ssDNA viruses (Table 1). Viruses associated with Magnoliopsida were the second most abundant group, with the vast majority classified as +ssRNA viruses (98.3%). Avian-associated viruses exhibited a higher proportion of ssDNA viruses (40.7%) alongside +ssRNA viruses (24.1%). Insect-associated viruses comprised 62 assemblies, with +ssRNA viruses representing the highest proportion (71%). Beyond these groups, assembly counts declined markedly, with *Liliopsida* (27 assemblies), environmental source hosts (18), *Malacostraca* (8), *Arachnida* (7), *Actinopterygii, Bivalvia*, and Angiosperms (3 each), *Squamata* (2), and *Ichthyosporea, Amphibia, Copepoda, Anthozoa*, and *Mamiellophyceae* (one each).

3.4. Non-human mammalian virus occurrences

We examined virus species occurrence across cities for the most prevalent host groups: non-human mammals, birds, dicot plants, and insects. If the same virus species had different accessions associated with different hosts, detections were counted separately for each host rather than assigning the entire virus species to a single host. Heatmaps show normalised read counts (RPKMF); however, because most viruses were rare, statistical analyses focused on presence/absence patterns, which are less sensitive to technical variation than quantitative abundance estimates.

Within non-human mammals, we analysed *Rodentia, Carnivora* (mainly cat and dog viruses), and *Artiodactyla* (mainly pig and cattle viruses).

In total, 31 unique rodent-associated virus species were detected, of which 14 occurred in at least five samples (Fig. 4A). The most prevalent viruses included hepatitis E–associated viruses, represented by *Rocahepevirus ratti* (rat HEV) and hepatitis E virus (*Paslahepevirus*), as well as *Cardiovirus C* and *Cardiovirus B, Protoparvovirus rodent 2* (rat parvovirus) and *Protoparvovirus rodent 1* (H-1 parvovirus), *Rosavirus, Iotapapillomavirus 1*, rat minute virus, *Aichivirus A* (Kobuvirus A), *Mouse mastadenovirus B, Protoparvovirus 1* (mouse parvovirus 1 and minute virus of mice), *Dependoparvovirus rodent 2* (murine adeno-associated virus 1 and 2), and *Alphacoronavirus 1*, similar to canine coronavirus previously reported

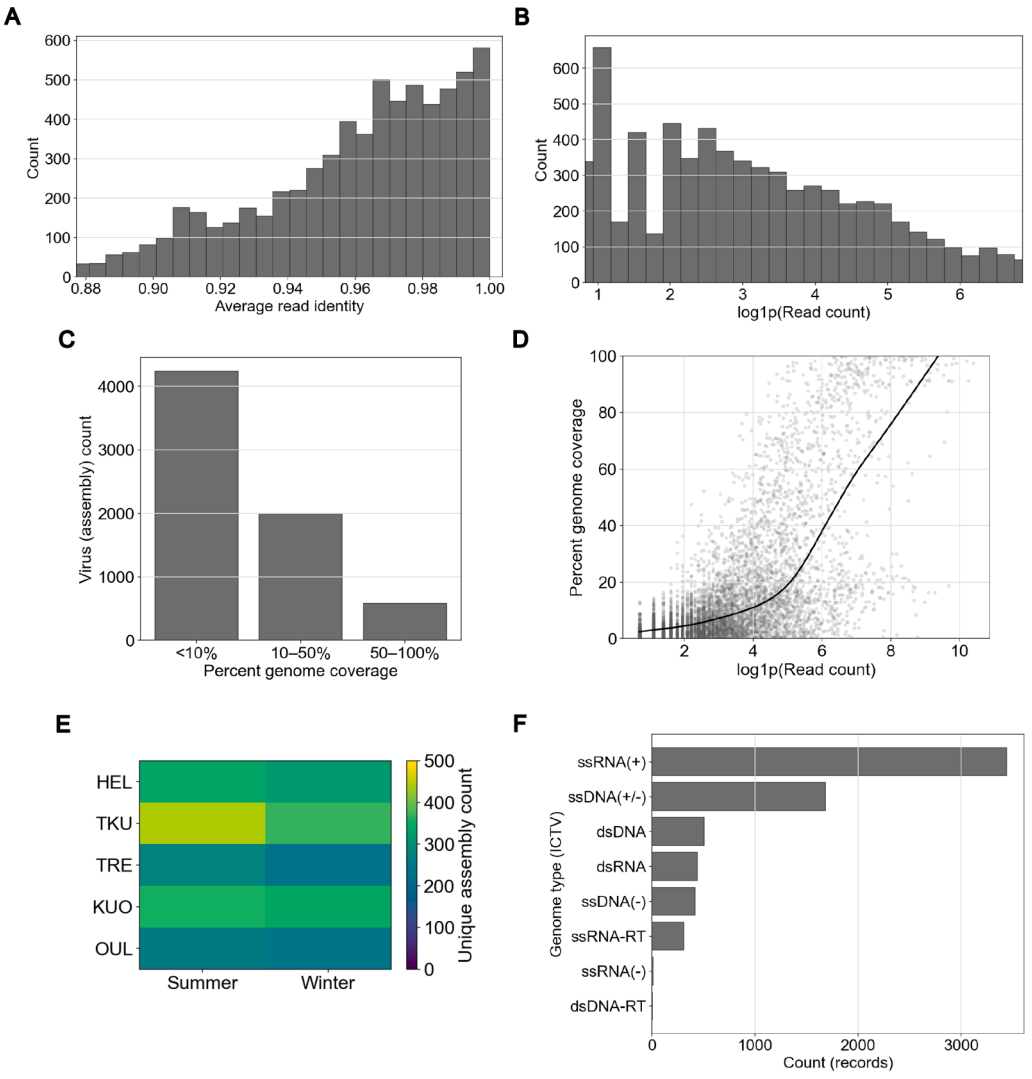

Fig. 3. Summary of non-human viral assemblies. (A) Average read identity. (B) log1p-transformed read counts per viral assembly. (C) Virus counts by percent assembly coverage (<10%, 10–50%, 50–100%). (D) Percent assembly coverage versus log1p(read count) with smoothed trend, showing a strong positive correlation. (E) Unique viral assembly counts by location (HEL = Helsinki, TKU = Turku, TRE = Tampere, KUO = Kuopio, OUL = Oulu) and season (summer: April–September; winter: other months). (F) Viral genome types.

Table 1
Unique viral assemblies by host class and genome type. Values are assembly counts with row percentages in parentheses, and the final column shows total assemblies per host class. Genome types grouped according to Baltimore classification, RT= reverse transcription.

Host class	dsDNA	dsDNA-RT	dsRNA	ssDNA(±)	ssDNA(-)	ssRNA(+)	ssRNA(-)	ssRNA-RT	Total
***Mammalia* (non-human)**	63 (9.6%)	2 (0.3%)	33 (5.0%)	165 (25.2%)	63 (9.6%)	310 (47.3%)	4 (0.6%)	16 (2.4%)	656
Magnoliopsida				1 (0.6%)		175 (98.3%)		2 (1.1%)	178
Aves	9 (5.6%)	1 (0.6%)	2 (1.2%)	66 (40.7%)	4 (2.5%)	39 (24.1%)	5 (3.1%)	36 (22.2%)	162
Insecta	1 (1.6%)		2 (3.2%)	15 (24.2%)		44 (71.0%)			62
Liliopsida			2 (7.4%)	1 (3.7%)		24 (88.9%)			27
Environmental source				12 (66.7%)		6 (33.3%)			18
Malacostraca			1 (12.5%)	6 (75.0%)		1 (12.5%)			8
Arachnida				2 (28.6%)		5 (71.4%)			7
Actinopterygii	1 (33.3%)		1 (33.3%)					1 (33.3%)	3
Bivalvia				2 (66.7%)		1 (33.3%)			3
Angiosperms						3 (100.0%)			3
Squamata	1 (50.0%)			1 (50.0%)					2
Ichthyosporea				1 (100.0%)					1
Amphibia						1 (100.0%)			1
Copepoda							1 (100.0%)		1
Anthozoa				1 (100.0%)					1
Mamiellophyceae			1 (100.0%)						1

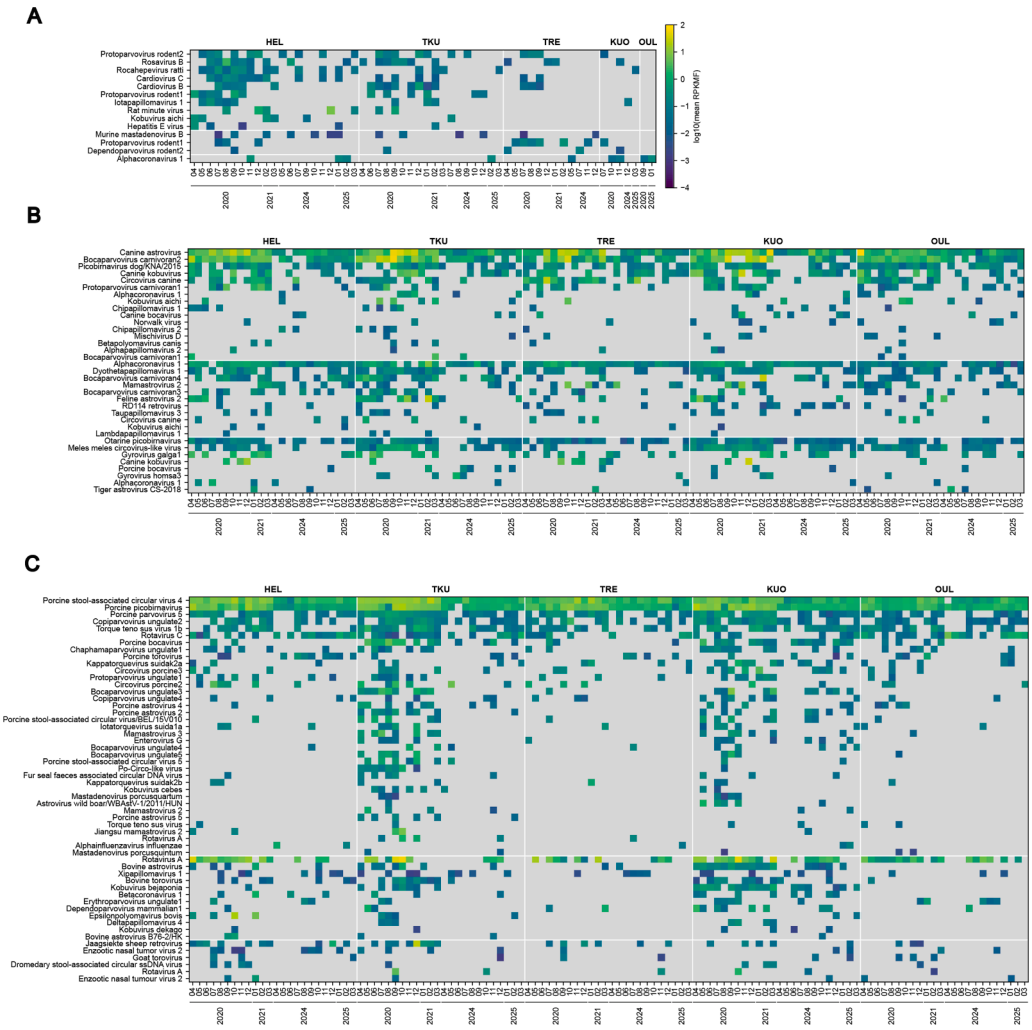

Fig. 4. Heatmap showing non-human mammalia-associated viruses across host genera and sampling locations. Rows represent viral taxa detected in hosts belonging to the orders (A) Rodentia, grouped by host genus *Rattus, Mus*, and other; (B) Carnivora, grouped by *Canis, Felis*, and other; and (C) Artiodactyla, grouped by *Sus, Bos*, and other. Host groups are separated by white lines. Columns represent sampling events defined by location (HEL, TKU, TRE, KUO, OUL) and month–year, with locations separated by white lines. Cell colour indicates the $\log_{10}$-transformed mean abundance (RPKMF) within each location–time combination, ranging from −4 to 2; light grey denotes no detection. Only viruses detected in at least five independent samples are shown. Rows are ordered within each host genus by prevalence and total abundance, and columns by location and sampling time.

from Chinese bamboo rat. The heatmap suggested a south–north gradient in rodent virus occurrence, with Helsinki showing the highest occurrence of rodent—particularly rat—viruses, whereas the northernmost city, Oulu, showed only two detections of Alphacoronavirus 1. Pairwise PERMANOVA tests based on presence/absence data indicated that the southern cities Helsinki, Turku, and Tampere differed significantly from Kuopio and Oulu (pseudo-F = 2.56–20.79, p_adj ≤ 0.0443; Table S2). However, within-location dispersion also differed significantly among cities (PERMDISP test; F = 12.37, p = 0.001), reflecting substantial variation in viral richness and sample-to-sample heterogeneity across locations.

Geographic differences reflected variation in rodent virus composition and within-city variability.

Out of 51 *Carnivora*-associated virus species detected, 36 occurred in at least five samples (Fig. 4B). The most prevalent dog-associated viruses were canine astrovirus, *Bocaparvovirus carnivoran 2*, picovirnavirus dog/KNA/2015, canine kobuvirus, and canine circovirus. Less frequent detections included *Protoparvovirus carnivoran 1, Alphacoronavirus 1, Aichivirus A, Chipapillomavirus 1* and *Chipapillomavirus 2*, canine bocavirus, Norwalk virus, *Mischivirus D*, and *Betapolyomavirus carnivoran 1*. The most prevalent cat-associated viruses were *Alphacoronavirus 1, Dyothetapapillomavirus 1*, and *Bocaparvovirus carnivoran 4*, whereas *Mamastrovirus 2, Bocaparvovirus carnivoran 2*, feline astrovirus 2, RD114 retrovirus, *Taupapillomavirus 2*, canine circovirus, *Aichivirus A*, and *Lambdapapillomavirus 1* occurred less frequently. In the "other Carnivora" group, otarine picovirnavirus (California sea lion) and Meles meles circovirus-like virus (European badger) were most common, while sporadic detections included gyroviruses from European polecat, canine kobuvirus from red fox, porcine bocavirus from *Mustela spp., Alphacoronavirus 1* from red fox and common raccoon dog, and tiger astrovirus CS-2018. Visually, the heatmap patterns (Fig. 4B) appeared broadly similar across locations; however, pairwise PERMANOVA test indicated moderate but uneven city-level structuring of *Carnivora*-associated virus assemblages. After multiple-testing correction and using a stringent significance threshold (p ≤ 0.01), only Tampere differed significantly from Turku and Kuopio (pseudo-F = 2.89–3.37, p_adj ≤ 0.005; Table S3). Using a less stringent threshold (p ≤ 0.05), Tampere also differed from Oulu, and Kuopio differed from Helsinki and Oulu (pseudo-F = 2.06–2.34, p_adj ≤ 0.044). In contrast, Helsinki did not differ significantly from Turku, Tampere, or Oulu, and Turku–Oulu comparisons were non-significant. Within-location dispersion did not differ among cities (PERMDISP; F = 0.21, p = 0.934), indicating comparable variability in *Carnivora*-associated viral communities within each location.

Out of 121 even-toed ungulate (*Artiodactyla*)–associated virus species detected, 54 occurred in at least five samples (Fig. 4C). In pigs, the most prevalent viruses were porcine stool–associated circular virus 4, porcine picobirnavirus, porcine parvovirus 5, *Copiparvovirus ungulate 2*, torque teno sus virus 1b, and rotavirus C. An additional 31 porcine virus species were detected sporadically, including bocaparvoviruses, circoviruses, astroviruses, torovirus, torque teno viruses, mamastroviruses, kobuvirus, copiparvovirus, enterovirus G, mastadenovirus, influenza virus, and rotavirus A. In cattle, rotavirus A was the most prevalent virus, followed by bovine astrovirus, whereas *Zetapapillomavirus 1*, bovine torovirus, kobuvirus, *Betacoronavirus 1*, erythroparvovirus, dependoparvovirus, epsilon polyomavirus, and deltapapillomavirus were detected infrequently. Additional Artiodactyla-associated viruses included Jaagsiekte sheep retrovirus, goat enzootic nasal tumor virus 2, dromedary stool–associated circular ssDNA virus, and rotavirus A from domestic sheep. Visually, the heatmap suggested separation of Turku and Kuopio from the other cities in *Artiodactyla*-associated virus occurrence. Consistent with this, PERMANOVA with multiple-testing correction showed that nearly all city pairs differed significantly, with particularly strong differentiation among Kuopio and Turku, which differed from most other cities (pseudo-$F = 5.03–6.59$, $p_adj \leq 0.0033$; Table S4). In contrast, Turku–Kuopio, Helsinki–Tampere, and Helsinki–Oulu differences were significant only at the $p \leq 0.05$ threshold (pseudo-$F = 1.99–2.27$, $p_adj \leq 0.0125$), while the Tampere–Oulu comparison was not significant (Table S4). Within-location dispersion also differed significantly among cities (PERMDISP; $F = 3.13$, $p = 0.015$), indicating that locations varied in the degree of sample-to-sample heterogeneity in virus presence/absence. Geographic structuring of artiodactyl-associated viral communities was associated with differences in community composition and within-location variability.

3.5. Dicot virus occurrences

Out of 89 dicot (*Magnoliopsida*)-associated virus species detected, 54 occurred in at least five samples (Fig. 5A). Within host groups, the most prevalent viruses were cucumber green mottle mosaic virus and cucurbit aphid-borne yellows virus in *Cucumis*, pepper mild mottle virus in *Capsicum*, tomato brown rugose fruit virus and tomato mosaic virus in *Solanum*, carrot red leaf virus in *Daucus*, aphid-borne yellows virus in *Cucurbita*, and turnip yellows virus in other dicot hosts. Other dicot-associated viruses occurred sporadically. Notably, three EU-regulated non-quarantine pests were detected, including the prevalent tomato brown rugose fruit virus, as well as *Nepovirus rubi* and *Nepovirus arabis*, all of which were present in samples from every city. In addition, the EU quarantine pest *Nepovirus lycopersici* was detected in all cities except Oulu. Other widely recognised agricultural pathogens included cucumber green mottle mosaic virus, pepper mild mottle virus, tomato mosaic virus, potato leafroll virus, and turnip yellows virus. Pairwise PERMANOVA based on presence/absence data showed no statistically significant differences in dicot-associated viral community composition between cities after multiple-testing correction ($p_adj \geq 0.05$ for all comparisons; Table S7). Within-location dispersion also did not differ significantly among cities (PERMDISP; $F = 0.37$, $p = 0.808$). Thus, *Magnoliopsida*-associated viral communities were broadly homogeneous across locations, with no evidence of spatial structuring.

3.6. Avian virus occurrences

Out of 52 avian virus species detected, 20 occurred in at least five samples (Fig. 5B). Among chicken-associated viruses, avian leukosis virus, chicken anemia virus (*Gyrovirus chickenanemica*), and *Gyrovirus galga 1* were detected in most samples. In contrast, *Mardivirus gallidalpha*

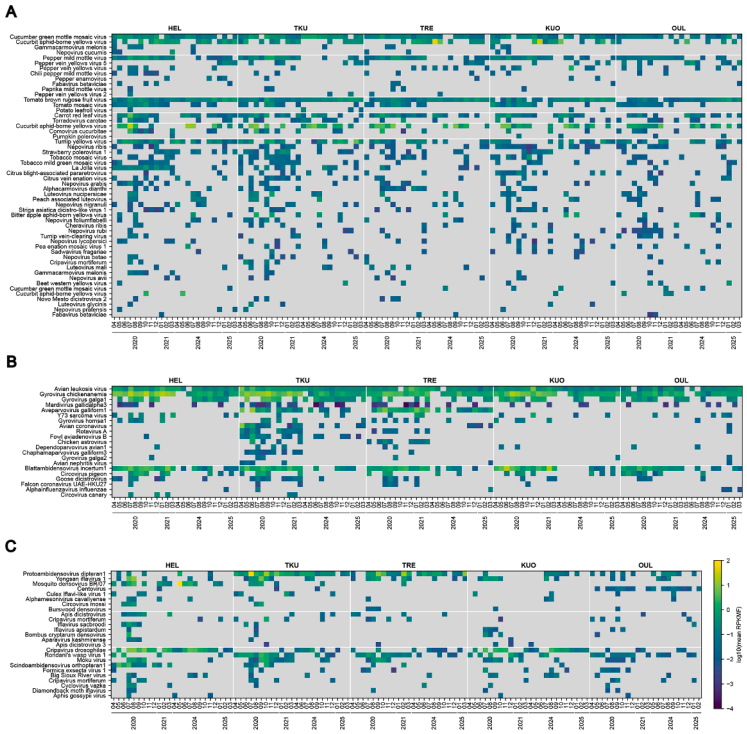

Fig. 5. Heatmap showing dicot-, bird-, and insect-associated viruses across host genera and sampling locations. Rows represent viral taxa detected in hosts belonging to the orders (A) Magnoliopsida, grouped by host genus *Cucumis, Capsicum, Solanum, Daucus, Cucurbita*, and other; (B) Aves, grouped by host genus *Gallus* and other; and (C) Insecta, grouped by host genus *Culex, Apis*, and other. Host groups are separated by white lines. Columns represent sampling events defined by location (HEL, TKU, TRE, KUO, OUL) and month–year, with locations separated by white lines. Cell colour indicates the $\log_{10}$-transformed mean abundance (RPKMF) within each location–time combination, ranging from −4 to 2; light grey denotes no detection. Only viruses detected in at least five independent samples are shown. Rows are ordered within each host genus by prevalence and total abundance, and columns by location and sampling time.

3, Galliform aveparvovirus 1, Y73 sarcoma virus, avian coronavirus, rotavirus A, fowl aviadenovirus B, chicken astrovirus, *Dependoparvovirus galliform 3, Gyrovirus galga 2*, and avian nephritis virus were either largely restricted to Turku or showed scattered occurrence across cities. Among non-galliform bird viruses, *Blattambidensovirus incertum 1* from great tit was the most prevalent, whereas circovirus pigeon, goose dicistrovirus, falcon coronavirus, circovirus canary, and alphainfluenza viruses originally isolated from turkey, finch, gull, and duck were detected sporadically. Visually, the heatmap indicated that Turku and Tampere harboured a higher frequency of chicken-associated viruses compared with the other cities. Consistent with this pattern, pairwise PERMANOVA after multiple-testing correction showed that Turku and Tampere differed significantly from Helsinki, Kuopio, and Oulu, as well as from each other (pseudo-$F = 3.84–8.48$, $p_adj = 0.0014$), whereas Kuopio–Oulu, Helsinki–Kuopio, and Helsinki–Oulu comparisons were not significant (Table S5). Within-location dispersion did not differ significantly among cities (PERMDISP; $F = 1.50$, $p = 0.166$), indicating comparable sample-to-sample variability of avian viral communities within each location.

3.7. Insect virus occurrences

Out of 44 insect-associated virus species detected, 25 occurred in at least five samples (Fig. 5C). The most frequent mosquito (*Culex*)–associated viruses were *Protoambidensovirus dipteran 1, Yongsan iflavirus 1*, and mosquito densovirus BR/07, whereas Centovirus, Culex iflavi-like virus 1, *Alphamesonivirus cavallyense*, Circovirus mossi, and Burswood densovirus were detected less frequently. Bee-associated viruses were generally more scattered across samples and included *Apis dicistrovirus, Cripavirus mortiferum, Iflavirus sacbroodi, Iflavirus apistardum, Bombus cryptarum densovirus, Aparavirus kashmirense*, and *Apis dicistrovirus 3*. Other insect viruses included frequently detected *Cripavirus drosophila*, Rondoni's wasp virus 1, and Moku virus from wasp, while rarer detections included *Scindoambidensovirus orthopteran 1* (house cricket), *Formica exsecta* virus (narrow-headed ant), Big Sioux River virus 1 (black bean aphid), *Cripavirus mortiferum* (pea aphid), *Cyclovirus vazka* (blue-eyed darner), diamondback moth iflavirus, and *Aphis gossypii virus* (cotton aphid). Visually, insect virus occurrence patterns appeared sparse and heterogeneous across cities, yet pairwise PERMANOVA revealed strong and widespread city-level structuring of insect-associated virus assemblages. After multiple-testing correction, all city pairs differed significantly, with the sole exception of the Turku–Tampere comparison (pseudo-$F = 3.10–7.96$, $p_adj \leq 0.0056$; Table S6). Within-location dispersion did not differ significantly among cities (PERMDISP; $F = 0.80$, $p = 0.43$), indicating comparable sample-to-sample variability of Insecta-associated viral communities within each location. Insect-associated viral communities showed strong spatial structuring driven by community composition.

4. Discussion

The viral diversity observed in this study reflects the methodological framework used, namely a targeted enrichment panel and reference genome database designed to recover human and non-human viral pathogens from pellet fraction of wastewater. Within this targeted dataset, wastewater viral diversity spanned multiple host groups, with most recovered viral sequences assigned to human-associated viruses. Consequently, non-human viruses were generally detected at low abundance and with limited genome coverage. The most common inferred hosts were non-human mammals, dicots, birds, and insects. Heatmap-based comparisons and pairwise PERMANOVA revealed clear city-level differences for viruses associated with *Rodentia, Artiodactyla, Aves*, and *Insecta*. In contrast, *Carnivora* showed weaker and less consistent distributional patterns, and no spatial variation was detected for Magnoliopsida. PERMDISP results indicated that, for rodents, even-toed ungulates, and chickens cities differed both in viral composition and in within-city variability, suggesting differences in the consistency of viral representation across sampling sites.

Distinct host-structured viral signals were observed in wastewater across geographic regions. Spatial variation was most pronounced for rodent-associated viruses. The largest and southernmost catchment, Helsinki, showed common rodent viruses in 20 of 24 samples, whereas the northernmost area, Oulu, showed such viruses in only two samples. This pattern is consistent with broader evidence that urban rodent abundance varies with city size, climate, and urbanisation, and that the occurrence of rodent viruses in wastewater reflects rodent presence within sewer systems (Richardson et al., 2025; Tsai et al., 2024). Although most detected rodent-associated viruses are considered host-restricted, zoonotic hepatitis viruses, including *Rocahepevirus ratti* and *Hepatitis E* virus, were also frequently detected.

The pronounced enrichment of *Artiodactyla*-associated viruses in Turku and Kuopio is consistent with regional differences in agricultural activity and food-system inputs rather than household food consumption alone. As livestock farm waste does not typically enter municipal sewer systems directly in Finland, these signals most likely reflect indirect inputs associated with agricultural and food-production activities. Livestock statistics from the Natural Resources Institute Finland indicate that pig production is present only in the Turku region, which also accounts for approximately 20% of the cattle population (Fig. S1). This background information aligns with the high frequency and diversity of pig- and cow-associated viruses observed in wastewater samples from the Turku region. In contrast, the Kuopio region accounts for approximately 50% of the cattle population across the study areas but has no registered pig farms; pig-associated viral signals in this region may therefore reflect inputs from local meat-processing facilities handling pig products (Finnish Food Authority, 2026). Important veterinary pathogens detected included rotavirus A and C, influenza A virus, bovine coronavirus (*Betacoronavirus 1*), Jaagsiekte sheep retrovirus, and goat enzootic nasal tumor virus 2 (De las Heras et al., 2003; Hofacre and Fan, 2010; Kostanić et al., 2024; Vincent et al., 2014). Together, these findings demonstrate host-structured viral signals in wastewater across geographic regions.

The *Carnivora*-associated virome was dominated by host-specific enteric and respiratory viruses typical of domestic dogs and cats, including several recognised pathogens: alphacoronaviruses (canine and feline coronaviruses), *Protoparvovirus carnivoran 1* (canine parvovirus), canine and feline astroviruses, canine kobuvirus, and canine circovirus (Beikpour et al., 2025; Di Martino et al., 2019; Patel and Heldens, 2009; Yu et al., 2024). Sporadic detections of viruses associated with wild carnivores and marine mammals likely reflect environmental mixing, food-system inputs, detection in incidental hosts, or the presence of previously undescribed virus species. The weak spatial structuring observed for *Carnivora*-associated viruses may reflect relatively uniform pet-related inputs into wastewater. This interpretation is consistent with Finland's high prevalence of companion animal ownership, with approximately 25% of households owning a dog or a cat (Finnish Kennel Club, 2023; Statistics Finland, 2016).

The avian wastewater virome was dominated by chicken-associated viruses, which likely explains why Turku and Tampere differed significantly from the other cities. Poultry production statistics from the Natural Resources Institute Finland indicate that the wastewater catchment areas of Turku and Tampere account for approximately 90% and 10%, respectively, of the chicken population across the catchment areas compared (Fig. S2). This background distribution is consistent with the strong enrichment of chicken-associated viral signals observed in these cities. Detected avian viruses included several recognised poultry pathogens (Fandiño et al., 2023; Fatoba and Adeleke, 2019; Otto et al., 2012; Rafique et al., 2024; Yugo et al., 2016). The most prevalent species were avian leukosis virus and chicken anemia virus (*Gyrovirus chickenanemia*), while avian coronavirus, fowl aviadenovirus, and rotavirus A were detected more sporadically. Interestingly, *Gallid alphaherpesvirus 3* was frequently detected but at very low levels, likely reflecting

vaccination practices against Marek's disease in commercial poultry (Gimeno et al., 2016). In addition, five influenza A virus detections were observed, one of which was classified as an avian influenza H5 subtype.

Across samples, insect-associated viral signals were dominated by recurrent mosquito-associated viruses, with additional repeated detections from bees and plant-feeding insects, particularly aphids, and *Drosophila*. Mosquitoes can propagate in sewers and remain active during winter (Hesson et al., 2016; Treskova et al., 2025), which may explain the year-round detection of *Culex*-associated viruses. Bee-associated viruses were generally scattered across samples and included several economically important pathogens with global distribution, such as sacbrood virus (*Iflavirus sacbroodi*), Kashmir bee virus (*Aparavirus kashmirense*), and slow bee paralysis virus (*Iflavirus apistardum*) (Lannutti et al., 2022).

Dicot-associated plant viruses were consistently detected across all cities with no measurable spatial structuring, reflecting widespread and uniform inputs of plant-derived material into wastewater. Most detected viruses were associated with commonly consumed crops; however, the broad host ranges of many plant viruses complicate source attribution in wastewater-based surveillance. Wastewater viromics captured four EU-regulated plant pathogens: the non-quarantine pests Arabis mosaic virus (*Nepovirus arabis*), Raspberry ringspot virus (*Nepovirus rubi*), and Tomato brown rugose fruit virus, and the quarantine pest Tomato ringspot virus (*Nepovirus lycopersici*). The latter was detected in 16 samples and is not reported in Finland according to the European and Mediterranean Plant Protection Organization (EPPO) distribution database. Tomato brown rugose fruit virus was officially reported for the first time in Finland in 2022 (EPPO, 2022), despite being highly prevalent in wastewater as early as 2020-21, with detections in 53 of 60 samples. Although this virus was not specifically targeted by the enrichment panel, its recovery is consistent with shotgun metagenomic study reporting widespread occurrence of tobamoviruses, including Tomato brown rugose fruit virus and Pepper mild mottle virus, in wastewater (Worp et al., 2025). Similar early detection of this virus in wastewater prior to official reporting has been described in Canada, Greece, and Italy (Worp et al., 2025). These findings highlight the early-warning potential of wastewater surveillance, although wastewater data alone cannot determine the source of detected viral material.

Wastewater viromics can capture host-specific occurrence patterns and provide early warning signals for animal and plant pathogens at the population level. The conclusions of this study are based on the occurrence of viral sequence signatures associated with particular host groups rather than definitive identification of actively circulating viruses within those hosts. Furthermore, because wastewater integrates multiple inputs, the source pathway of individual viral detections cannot be currently resolved from sequence data alone. Host attribution based on sequence similarity is nevertheless inherently uncertain, as viruses may be detected outside their typical or locally expected host range; for example, viruses annotated as associated with tiger or dromedary likely reflect similarity to viruses characterised elsewhere rather than the local presence of these hosts in Finnish wastewater catchments. In some cases, host assignments reflect the host associated with the reference accession rather than the canonical host range of the viral species. In addition, the targeted enrichment panel and reference database used in this study contributed to the higher recovery of human-associated viruses. Accordingly, the non-human viral sequences were generally detected at low abundance, most covering less than 10% of the target genome, which limits taxonomic resolution and increases uncertainty in host assignment. Although the mapping-based EsViritu workflow enables sensitive detection of viral sequence signatures at low genome coverage, addressing these limitations through improved genome recovery is essential for applying wastewater surveillance to veterinary and agricultural pathogen monitoring.

5. Conclusion

Our results corroborate with previous studies showing that wastewater surveillance captures viruses associated with pets, synanthropic wildlife, livestock, and plants. We further demonstrate that the occurrence of host-associated viruses reflects host presence, such that regions with established host populations—such as large urban rodent populations or areas with livestock production—show consistent detection of corresponding viral signals, whereas regions lacking these hosts show little or no detection. Overall, wastewater surveillance of animal and plant pathogens is already feasible and, with methodological refinement, can become a robust component of One Health–oriented surveillance.

CRediT authorship contribution statement

Jaana Jurvansuu: Conceptualization, Formal analysis, Visualization, Writing – original draft, Writing – review & editing. **Eevi Sipponen:** Formal analysis, Investigation, Visualization, Writing – review & editing. **Elisa Salmivirta:** Investigation. **Kirsi-Maarit Lehto:** Conceptualization, Writing – review & editing. **Aki Havulinna:** Conceptualization, Writing – review & editing. **Tarja Pitkänen:** Conceptualization, Funding acquisition, Writing – review & editing. **Sami Oikarinen:** Conceptualization, Funding acquisition, Supervision, Writing – review & editing.

Declaration of competing interest

K.M.L. and S.O. are board members of GreenSeq Ltd. The other authors declare that they have no known competing financial interests or personal relationships that could have appeared to influence the work reported in this paper.

Acknowledgements

We thank Mirka Halonen, Minta Lumme, and Janna Uuttu for laboratory assistance, wastewater treatment plant personnel for sampling and metadata, and CSC – IT Center for Science, Finland for computing resources. T.P. acknowledges funding from the Finnish Government supplementary budget for COVID-19 research, the Ministry of Agriculture and Forestry [grant number 4400T-0807], and the Research Council of Finland [grant number 355355]. S.O. acknowledges funding from the Research Council of Finland [grant number 355135].

Supplementary materials

Supplementary material associated with this article can be found, in the online version, at doi:10.1016/j.watres.2026.126485.

Data availability

We have shared the links to our data and code at the manuscript text.

References

Adriaenssens, E.M., Farkas, K., McDonald, J.E., Jones, D.L., Allison, H.E., McCarthy, A.J., 2021. Tracing the fate of wastewater viruses reveals catchment-scale virome diversity and connectivity. Water Res. 203, 117568. https://doi.org/10.1016/j.watres.2021.117568.

Al-Gheethi, A., Ma, N.L., Rupani, P.F., Sultana, N., Yaakob, M.A., Mohamed, R., Soon, C. F., 2023. Biowastes of slaughterhouses and wet markets: an overview of waste management for disease prevention. Environ. Sci. Pollut. Res. Int. 30 (28), 71780–71793. https://doi.org/10.1007/s11356-021-16629-w.

Beikpour, F., Letafati, A., Fakhr, Z.A., Decaro, N., Mozhgani, S.-H., 2025. Canine circovirus: an emerging virus of dogs and wild canids. Ir. Vet. J. 78 (1), 5. https://doi.org/10.1186/s13620-025-00290-7.

Bibby, K., Peccia, J., 2013. Identification of viral pathogen diversity in sewage sludge by metagenome analysis. Environ. Sci. Technol. 47 (4), 1945–1951. https://doi.org/10.1021/es305181x.

Chahal, C., van den Akker, B., Young, F., Franco, C., Blackbeard, J., Monis, P., 2016. Pathogen and particle associations in wastewater: significance and implications for treatment and disinfection processes. Adv. Appl. Microbiol. 97, 63–119. https://doi.org/10.1016/bs.aambs.2016.08.001.

Clark, J.R., Terwilliger, A., Avadhanula, V., Tisza, M., Cormier, J., Javornik-Cregeen, S., Ross, M.C., Hoffman, K.L., Troisi, C., Hanson, B., Petrosino, J., Balliew, J., Piedra, P. A., Rios, J., Deegan, J., Bauer, C., Wu, F., Mena, K.D., Boerwinkle, E., Maresso, A.W., 2023. Wastewater pandemic preparedness: toward an end-to-end pathogen monitoring program. Front. Public Health 11, 1137881. https://doi.org/10.3389/fpubh.2023.1137881.

Cock, P.J., Antao, T., Chang, J.T., Chapman, B.A., Cox, C.J., Dalke, A., Friedberg, I., Hamelryck, T., Kauff, F., Wilczynski, B., de Hoon, M.J., 2009. Biopython: freely available Python tools for computational molecular biology and bioinformatics. Bioinformatics 25 (11), 1422–1423. https://doi.org/10.1093/bioinformatics/btp163.

Crank, K., Chen, W., Bivins, A., Lowry, S., Bibby, K., 2022. Contribution of SARS-CoV-2 RNA shedding routes to RNA loads in wastewater. Sci. Total Environ. 806, 150376. https://doi.org/10.1016/j.scitotenv.2021.150376.

De las Heras, M., Ortín, A., Cousens, C., Minguijón, E., Sharp, J.M., 2003. Enzootic nasal adenocarcinoma of sheep and goats. Curr. Top. Microbiol. Immunol. 275, 201–223. https://doi.org/10.1007/978-3-642-55638-8_8.

Di Martino, B., Di Profio, F., Melegari, I., Marsilio, F., 2019. Feline virome-a review of novel enteric viruses detected in cats. Viruses 11, 908. https://doi.org/10.3390/v11100908.

dos Santos, D.R., de Paula, V.S., de Oliveira, J.M., Marchevsky, R.S., Pinto, M.A., 2011. Hepatitis E virus in swine and effluent samples from slaughterhouses in Brazil. Vet. Microbiol. 149 (1-2), 236–241. https://doi.org/10.1016/j.vetmic.2010.10.024.

Duarte, M.F., de Andrade, I.A., Silva, J.M.F., de Melo, F.L., Machado, A.M., Inoue-Nagata, A.K., Nagata, T., 2023. Metagenomic analyses of plant virus sequences in sewage water for plant viruses monitoring. Trop. Plant Pathol. 48, 408–416. https://doi.org/10.1007/s40858-023-00575-8.

European and Mediterranean Plant Protection Organization (EPPO), 2022. First report of tomato brown rugose fruit virus in Finland. EPPO Reporting Service No. 08, 2022. Available at: (accessed 16 July 2026) https://gd.eppo.int/reporting/article-7399.

Fandiño, S., Gomez-Lucia, E., Benítez, L., Doménech, A., 2023. Avian Leukosis: will we be able to get rid of it? Anim. (Basel) 13, 2358. https://doi.org/10.3390/ani13142358.

Fatoba, A.J., Adeleke, M.A., 2019. Chicken anemia virus: a deadly pathogen of poultry. Acta Virol. 63 (1), 19–25. https://doi.org/10.4149/av_2019_110.

Finnish Food Authority, 2026. Approved establishments handling meat products. Finnish Food Authority, Helsinki, Finland. Available at: http://www.ruokavirasto.fi/en/foodstuffs/food-sector/setting-up-a-food-business/make-an-announcement-of-a-food-business-or-apply-for-an-approval/approved-establishments/. (accessed 10 April 2026).

Finnish Kennel Club, 2023. Uusi koirakanta-arvio kertoo: suomessa on yli 800 000 koiraa, joista yli 580 000 on Suomen kennelliiton rekisterissä. https://www.kennelliitto.fi/tietoa-meista/uutiset/uusi-koirakanta-arvio-kertoo-suomessa-yli-800-000-koiraa-joista-yli-580-000-suomen-kennelliiton-rekisterissa.

Firth, C., Bhat, M., Firth, M.A., Williams, S.H., Frye, M.J., Simmonds, P., Conte, J.M., Ng, J., Garcia, J., Bhuva, N.P., Lee, B., Che, X., Quan, P.L., Lipkin, W.I., 2014. Detection of zoonotic pathogens and characterization of novel viruses carried by commensal Rattus norvegicus in New York City. mBio 5 (5). https://doi.org/10.1128/mBio.01933-14 e01933-01914.

Gimeno, I.M., Cortes, A.L., Faiz, N., Villalobos, T., Badillo, H., Barbosa, T., 2016. Efficacy of various HVT vaccines (Conventional and Recombinant) against Marek's disease in broiler chickens: effect of dose and age of vaccination. Avian Dis. 60 (3), 662–668. https://doi.org/10.1637/11415-040116-Reg.1.

Hesson, J.C., Schäfer, M.L., Lundström, J.O., 2016. First report on human-biting Culex pipiens in Sweden and Scandinavia. Parasites Vectors 9, 632. https://doi.org/10.1186/s13071-016-1925-3.

Himsworth, C.G., Parsons, K.L., Jardine, C., Patrick, D.M., 2013. Rats, cities, people, and pathogens: a systematic review and narrative synthesis of literature regarding the ecology of rat-associated zoonoses in urban centers. Vector. Borne Zoonotic. Dis. 13 (6), 349–359. https://doi.org/10.1089/vbz.2012.1195.

Hofacre, A., Fan, H., 2010. Jaagsiekte sheep retrovirus biology and oncogenesis. Viruses 2 (12), 2618–2648. https://doi.org/10.3390/v2122618.

Jones, D.L., Baluja, M.Q., Graham, D.W., Corbishley, A., McDonald, J.E., Malham, S.K., Hillary, L.S., Connor, T.R., Gaze, W.H., Moura, I.B., Wilcox, M.H., Farkas, K., 2020. Shedding of SARS-CoV-2 in feces and urine and its potential role in person-to-person transmission and the environment-based spread of COVID-19. Sci. Total Environ. 749, 141364. https://doi.org/10.1016/j.scitotenv.2020.141364.

Karatas, M., Bloemen, M., Swinnen, J., Roukaerts, I., Gucht, S.V., Van Ranst, M., Wollants, E., Matthijnssens, J., 2025. Untapped potential of wastewater for animal and potentially zoonotic virus surveillance: pilot study to detect non-human animal viruses in urban settings. Environ. Int. 199, 109500. https://doi.org/10.1016/j.envint.2025.109500.

Kitajima, M., Sassi, H.P., Torrey, J.R., 2018. Pepper mild mottle virus as a water quality indicator. NPJ Clean. Water 1 (1), 19. https://doi.org/10.1038/s41545-018-0019-5.

Kostanić, V., Kunić, V., Prišlin Šimac, M., Lolić, M., Sukalić, T., Brnić, D., 2024. Comparative insights into acute gastroenteritis in cattle caused by bovine rotavirus A and bovine coronavirus. Vet. Sci. 11 (12), 671. https://www.mdpi.com/2306-7381/11/12/671.

Lancaster, E., Winston, R., Martin, J., Lee, J., 2024. Urban stormwater green infrastructure: evaluating the public health service role of bioretention using microbial source tracking and bacterial community analyses. Water Res. 259, 121818. https://doi.org/10.1016/j.watres.2024.121818.

Lannutti, L., Gonzales, F.N., Dus Santos, M.J., Florin-Christensen, M., Schnittger, L., 2022. Molecular detection and differentiation of arthropod, fungal, protozoan, bacterial and viral pathogens of honeybees. Vet. Sci. 9, 221. https://doi.org/10.3390/vetsci9050221.

Li, G., Zhou, D., Zhao, M., Liu, Q., Hao, X., Yan, T., Yuan, S., Zhang, S., Cheng, Z., 2021. Kinetic analysis of pathogenicity and tissue tropism of gyrovirus 3 in experimentally infected chickens. Vet. Res. 52 (1), 120. https://doi.org/10.1186/s13567-021-00990-2.

Lopez-Roblero, A., Martínez Cano, D.J., Diego-García, E., Guillén-Navarro, G.K., Iša, P., Zarza, E., 2024. Metagenomic analysis of plant viruses in tropical fresh and wastewater. Environ. DNA 6 (1), e416. https://doi.org/10.1002/edn3.416.

Mallin, M.A., Johnson, V.L., Ensign, S.H., 2009. Comparative impacts of stormwater runoff on water quality of an urban, a suburban, and a rural stream. Environ. Monit. Assess. 159 (1-4), 475–491. https://doi.org/10.1007/s10661-008-0644-4.

Monteiro, S., Queiroz, G., Ferreira, F., Santos, R., 2021. Characterization of Stormwater runoff based on microbial source tracking methods [Original Research]. Front. Microbiol. 12, 674047. https://doi.org/10.3389/fmicb.2021.674047.

Mozzherin, D., 2025. GNverifier – a reconciler and resolver of scientific names against more than 100 data sources. https://doi.org/10.5281/zenodo.17245658. Version (v1.3.0).

Naccache, S.N., Hackett, J., Delwart, E.L., Chiu, C.Y., 2014. Concerns over the origin of NIH-CQV, a novel virus discovered in Chinese patients with seronegative hepatitis. Proc. Natl. Acad. Sci. 111 (11), E976. https://doi.org/10.1073/pnas.1317064111.

Naughton, C.C., Roman, F.A., Alvarado, A.G.F., Tariqi, A.Q., Deeming, M.A., Kadonsky, K.F., Bibby, K., Bivins, A., Medema, G., Ahmed, W., Katsivelis, P., Allan, V., Sinclair, R., Rose, J.B., 2023. Show us the data: global COVID-19 wastewater monitoring efforts, equity, and gaps. FEMS Microbes. 4, xtad003. https://doi.org/10.1093/femsmc/xtad003.

Otto, P.H., Ahmed, M.U., Hotzel, H., Machnowska, P., Reetz, J., Roth, B., Trojnar, E., Johne, R., 2012. Detection of avian rotaviruses of groups A, D, F and G in diseased chickens and turkeys from Europe and Bangladesh. Vet. Microbiol. 156 (1-2), 8–15. https://doi.org/10.1016/j.vetmic.2011.10.001.

Patel, J.R., Heldens, J.G., 2009. Review of companion animal viral diseases and immunoprophylaxis. Vaccine 27 (4), 491–504. https://doi.org/10.1016/j.vaccine.2008.11.027.

Rafique, S., Jabeen, Z., Pervaiz, T., Rashid, F., Luo, S., Xie, L., Xie, Z., 2024. Avian infectious bronchitis virus (AIBV) review by continent. Front. Cell Infect. Microbiol. 14, 1325346. https://doi.org/10.3389/fcimb.2024.1325346.

Richardson, J.L., McCoy, E.P., Parlavecchio, N., Szykowny, R., Beech-Brown, E., Buijs, J. A., Buckley, J., Corrigan, R.M., Costa, F., DeLaney, R., Denny, R., Helms, L., Lee, W., Murray, M.H., Riegel, C., Souza, F.N., Ulrich, J., Why, A., Kiyokawa, Y., 2025. Increasing rat numbers in cities are linked to climate warming, urbanization, and human population. Sci. Adv. 11 (5), eads6782. https://doi.org/10.1126/sciadv.ads6782.

Robins, K., Leonard, A.F.C., Farkas, K., Graham, D.W., Jones, D.L., Kasprzyk-Hordern, B., Bunce, J.T., Grimsley, J.M.S., Wade, M.J., Zealand, A.M., McIntyre-Nolan, S., 2022. Research needs for optimising wastewater-based epidemiology monitoring for public health protection. J. Water Health 20 (9), 1284–1313. https://doi.org/10.2166/wh.2022.026.

Sarekoski, A., Tiwari, A., Hokajärvi, A.-M., Kauppinen, A., Pitkänen, T., Savolainen-Kopra, C., Meriläinen, O., 2024. Simultaneous biomass concentration and subsequent quantitation of multiple infectious disease agents and antimicrobial resistance genes from community wastewater. Environ. Int. 191, 108973. https://doi.org/10.1016/j.envint.2024.108973.

Sayers, E.W., Beck, J., Brister, J.R., Bolton, E.E., Canese, K., Comeau, D.C., Funk, K., Ketter, A., Kim, S., Kimchi, A., Kitts, P.A., Kuznetsov, A., Lathrop, S., Lu, Z., McGarvey, K., Madden, T.L., Murphy, T.D., O'Leary, N., Phan, L., Ostell, J., 2020. Database resources of the national center for biotechnology information. Nucleic. Acids. Res. 48 (D1), D9–D16. https://doi.org/10.1093/nar/gkz899.

Secretariat, G., 2023. GBIF Backbone Taxonomy. Checklist Dataset. https://doi.org/10.15468/39omei.

Sherchan, S., Shahin, S., Alarcon, J., Brosky, H., Potter, C., Dada, A.C., 2022. Microbial source tracking of fecal contamination in stormwater runoff. J. Water Health 20 (9), 1271–1283. https://doi.org/10.2166/wh.2022.286.

Sidhu, J.P.S., Ahmed, W., Gernjak, W., Aryal, R., McCarthy, D., Palmer, A., Kolotelo, P., Toze, S., 2013. Sewage pollution in urban stormwater runoff as evident from the widespread presence of multiple microbial and chemical source tracking markers. Sci. Total Environ. 463-464, 488–496. https://doi.org/10.1016/j.scitotenv.2013.06.020.

Statistics Finland, 2016. Household Budget Survey 2016: Pet ownership in Finnish households. Statistics Finland. Retrieved 19.01 from. https://stat.fi/til/ktutk/2016/ktutk_2016_2016-11-03_tie_001_en.html.

Symonds, E.M., Rosario, K., Breitbart, M., 2019. Pepper mild mottle virus: agricultural menace turned effective tool for microbial water quality monitoring and assessing (waste)water treatment technologies. PLoS Pathog. 15 (4), e1007639. https://doi.org/10.1371/journal.ppat.1007639.

Thioulouse, J., Dray, S., Dufour, A.-B., Aurélie, S., Jombart, T., Pavoine, S., 2018. Multivariate Analysis of Ecological Data with ade4. https://doi.org/10.1007/978-1-4939-8850-1.

Tisza, M., Javornik Cregeen, S., Avadhanula, V., Zhang, P., Ayvaz, T., Feliz, K., Hoffman, K.L., Clark, J.R., Terwilliger, A., Ross, M.C., Cormier, J., Moreno, H., Wang, L., Payne, K., Henke, D., Troisi, C., Wu, F., Rios, J., Deegan, J., Maresso, A.W., 2023. Wastewater sequencing reveals community and variant dynamics of the collective human virome. Nat. Commun. 14 (1), 6878. https://doi.org/10.1038/s41467-023-42064-1.

Treskova, M., Montalvo, T., Rocklöv, J., Hatfield, C., Bartumeus, F., Dasgupta, S., Encarnação, J., Lowe, R., Semenza, J.C., Stiles, P., Noya, J., Valsecchi, A., Bärnighausen, T., Palmer, J.R.B., Bunker, A., 2025. Effects of mosquito-proofing storm drains on adult and larval mosquito abundance: protocol of the IDAlErt storm drAin randomiSed controlled trial (IDEAS). MethodsX 14, 103102. https://doi.org/10.1016/j.mex.2024.103102.

Tsai, K.-H., Yen, T.-Y., Tung, H.-H., Ho, A., Chien, Y.-T., Wang, C.-Y., Kang, S.-W., Juan, N.-N., Lin, F.-L., 2024. Surveillance of emerging rodent-borne pathogens in wastewater in taiwan: a one health approach. Trop. Med. Infect. Dis. 9 (11), 282. https://www.mdpi.com/2414-6366/9/11/282.

Vincent, A., Awada, L., Brown, I., Chen, H., Claes, F., Dauphin, G., Donis, R., Culhane, M., Hamilton, K., Lewis, N., Mumford, E., Nguyen, T., Parchariyanon, S., Pasick, J., Pavade, G., Pereda, A., Peiris, M., Saito, T., Swenson, S., Ciacci-Zanella, J., 2014. Review of influenza A virus in swine worldwide: a call for increased surveillance and research. Zoonoses. Public Health 61 (1), 4–17. https://doi.org/10.1111/zph.12049.

Worp, N., Nieuwenhuijse, D.F., Izquierdo-Lara, R.W., Schapendonk, C.M.E., Brinch, C., Jensen, E.E.B., Munk, P., Hendriksen, R.S., Møller, F.D., Petersen, T.N., Kjeldgaard, J.S., Svendsen, C.A., Bego, A., Power, P., Rees, C., Lambrinidis, D., Neilson, E.H.J., Gibb, K., Coventry, K., Global Sewage Surveillance, C., 2025. Unveiling the global urban virome through wastewater metagenomics. Nat. Commun. 16 (1), 10707. https://doi.org/10.1038/s41467-025-65208-x.

Yu, Y., Yao, Y., Shan, H., Han, X., 2024. Clinical detection of four emerging canine diarrhea-associated viruses and evolutionary analysis of canine kobuvirus. Arch. Virol. 169 (12), 242. https://doi.org/10.1007/s00705-024-06161-w.

Yugo, D.M., Hauck, R., Shivaprasad, H.L., Meng, X.J., 2016. Hepatitis virus infections in poultry. Avian Dis. 60 (3), 576–588. https://doi.org/10.1637/11229-070515-Review.1.

Zahedi, A., Monis, P., Deere, D., Ryan, U., 2021. Wastewater-based epidemiology—surveillance and early detection of waterborne pathogens with a focus on SARS-CoV-2, Cryptosporidium and Giardia. Parasitol. Res. 120 (12), 4167–4188. https://doi.org/10.1007/s00436-020-07023-5.

Zhang, Z., He, F., Yi, L., Deng, Z., Wang, R., Shen, L., Fu, S., 2024. Wastewater surveillance together with metaviromic data revealed the unusual resurgence of infectious diseases after the first wave of the COVID-19 outbreak. J. Hazard. Mater. 473, 134635. https://doi.org/10.1016/j.jhazmat.2024.134635.